Experimental study of a wave energy scavenging system onboard autonomous surface vessels (ASVs)

J. A. Bowker, N. C. Townsend, M. Tan, R. A. Shenoi
Fluid Structure Interactions Group, Faculty of Engineering and the Environment
University of Southampton
SO17 1BJ UK
jab1e08@soton.ac.uk

***Abstract*—Autonomous Surface Vehicles (ASV) have many potential applications in the maritime industry and ocean science. To subsist in the ocean space, an ASV must have the ability to scavenge energy from the surrounding environment. Waves are an abundant source of energy on the ocean surface and a suitable resource for an ASV to scavenge. Flapping foils have been shown to generate thrust in a wavy flow and power in a uniform flow. The aim of this experimental study is to investigate the relationship between flapping foil propulsion and power generation in the context of ASVs. Initial experiments incorporating fully passive flapping foils submerged at the bow and stern of a surface vessel in head waves were performed in a towing tank. The spring-loaded foils were located at the end of rigid pivot arms protruding at the bow and abaft of the vessel. The pivot arms were free to rotate about a location beneath the keel line and restrained by adjustable rotational dampers. In this free condition, wave energy is recovered in the form of work applied by the flapping foils through the rotary dampers which were used to simulate the damping effects of a power take-off device. Thrust was generated under conditions when the pivot arm was fixed. This system, referred to as the Flapping Energy Utilization and Recovery (FLEUR) system, could serve as a dual-purpose wave energy scavenging propulsor and power generator for long-endurance ASVs.**

I. Introduction

Efforts have been made to increase the longevity of the ASV deployment through the scavenging of marine energy resources. It is well-known that the marine environment is a particularly challenging domain to operate man-made systems in and steps to improve the reliability and energy scavenging capabilities of ASVs is required to achieve their full potential. The spectrum of current ASVs ranges from systems that have a high onboard power capacity for fast speeds and significant onboard capability through to long range endurance ASVs that harvest marine energy for propulsion and limited onboard powering. With the rapid developments in technology and the development of hybrid marine energy scavenging devices, it is expected that the aforementioned spectrum range of ASV capability versus endurance will narrow resulting in the long term deployment of highly capable ASVs [1], see Figure 1. The motivation for this research is to contribute to the attainment of ASV self-sustainability through the development of marine energy scavenging devices.

Wave energy is an abundant source of marine energy on the ocean surface, with 90% of high frequency waves storing an energy density of greater than 2kW/m [2]. This research is, therefore, focused on the utilization and recovery of wave energy for ASV propulsion and onboard energy harvesting.

Numerous autonomous marine vessels have been designed to utilize wave energy for direct propulsion. The Wave Glider, developed by Liquid Robotics, is passively propelled by a submerged set of foils, referred to as the 'glider', attached to a surface float via a tether [3]. As the float heaves in response to the ocean waves, the submerged glider heaved and plunged through the water. The resulting effective flow over the foils generates thrust that drives the float forward over the waves.

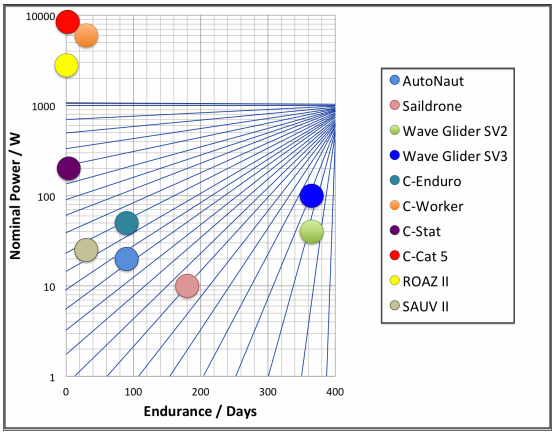

Figure 1: Convergence of ASV endurance and capability [3][4][5][6][7][8]

MOST (Autonomous Vessels) Ltd have also developed a long range endurance wave propelled ASV and have recently launched the commercial version called AutoNaut [7]. AutoNaut propels itself using the same technique patented and developed by Linden and Jakobsen respectively [9][10]. The vessel consists of two flapping foils, one at the bow and one at the stern, and propels itself using the wave induced vessel motions to generate thrust from spring-loaded foils. Using a similar method, Terao and Sakagami have developed a system called the Wave Devouring Propulsion System (WDPS), which is an ASV propelled using vessel induced motions to excite spring-loaded foils [11]. Research carried out by Townsend and Shenoi has investigated the use of a gyroscopic system to harvest wave energy onboard vessels through gyroscopic precession in response to the wave-induced vessel pitch and

978-1-4799-8736-8/15/$31.00 ©2015 IEEE

This is a DRAFT. As such it may not be cited in other works.
The citable Proceedings of the Conference will be published in
IEEE Xplore shortly after the conclusion of the conference.

roll. The study has been expanded to test the feasibility of using this gyroscopic system for recharging autonomous underwater vehicles (AUVs) at the sea surface [12].

The proposed Flapping Energy Utilization and Recovery (FLEUR) system presented in this paper is an expansion of previous work on spring-loaded wave devouring flapping foils, incorporating the capability of generating onboard power. The advantage of such a system is the ability to alter the mode of a remote ASV to either propulsion or power generation depending on the mission status.

II. Flapping Foil Thrust and Power Generation

Considerable theoretical and experimental studies have been carried out to investigate the characteristics of flapping foils and their suitability for potential applications. Isshiki uses the term 'wave devouring propulsion' to describe the mechanism of submerged flapping foils generating thrust in waves [13]. Wave devouring propulsion suitably describes the field of research from the initial theory presented by Wu and the theory developed by Grue et al. through to recent studies that investigate their application on-board ships [14][15][16]. Power generation from flapping foils is a more recent body of research, which has seen increased levels of interest due to its potential application as a more efficient flow energy harvesters when compared to their rotary counterparts such as tidal turbines[17].

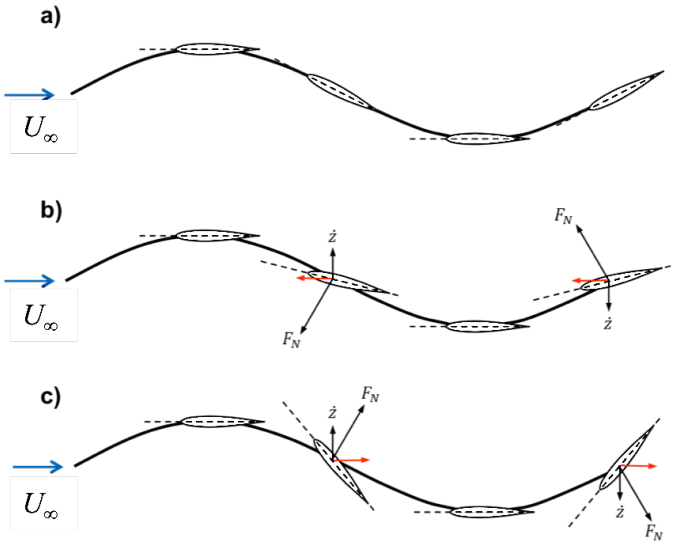

Figure 2: Flapping foil kinematics heaving and pitching in a steady flow; a) Feathering b) Thrust generation c) Power generation

Figure 2 shows the pathline of a flapping foil immersed in a constant flow stream, U_∞, with prescribed pitch and heave motions. The prescribed motion produces a response that is synonymous with either feathering, propulsion or power generation. The foil heave velocity, $\dot{z}$, contributes to the relative flow at the leading edge resulting in an effective angle of attack due to the foil motions, α_e. By defining the foil pitch (θ), the effective angle of attack is evaluated as follows:

$$\alpha_e = \theta - tan^{-1}(\frac{-\dot{z}}{U_\infty})$$

This relationship between the effective angle of attack and the foil motions defines the resultant hydrodynamic force. Depending on the flapping characteristics of the foil, the resultant hydrodynamic force will dictate the function of the system. Power is generated if the lift force in the vertical axis is synchronous with the foil heave velocity. This power provides the impetuous for the foil to heave as well as generating further power that can be harvested during the cycle. However, in this instance, drag develops over the cycle in the form of a Von Karman vortex street in the down-stream flow field [18]. Optimizing the flapping foil parameters for propulsion generates a hydrodynamic force with a horizontal component which exceeds the drag component to produce a net thrust. In this mode, the foil sheds a reverse Von Karman vortex street in the down-stream flow field that is indicative of a jet stream. The thrust can be evaluated by analyzing the change in momentum of the fluid, as depicted by Jones et al. in Figure 3.

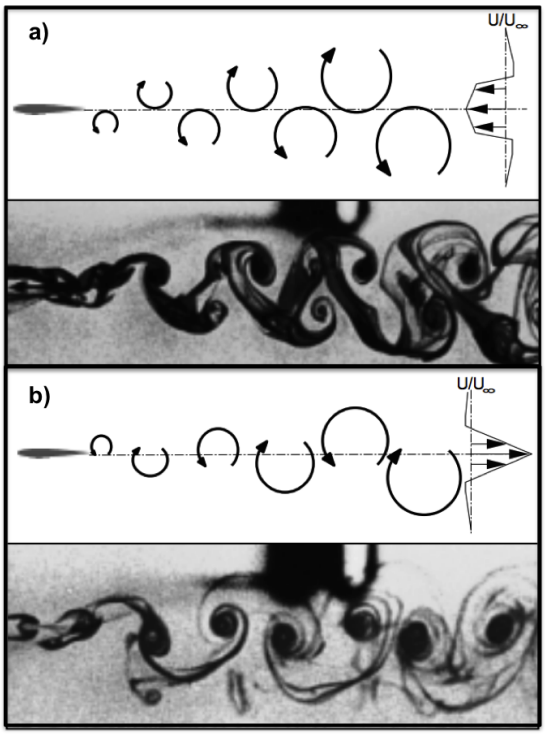

Figure 3: Down-stream flow field; a) Drag b) Thrust [18]

Previous studies have identified that the introduction of waves significantly contributes to the thrust generated by flapping foils. Immersing the flapping foil in a wavy flow introduces another velocity component to the system in the form of orbital particle motions in the fluid stream. In deep water, the profile of a regular wave can be modelled using linear wave theory, from which the velocity potential is differentiated to derive the horizontal and vertical wave orbital

particle velocities, u and v respectively. Further research has incorporated the analysis of fixed foils submerged beneath a surface vessel [16]. Coupling the wave induced vessel motions with that of a spring-loaded foil activates the flapping characteristics required for thrust generation.

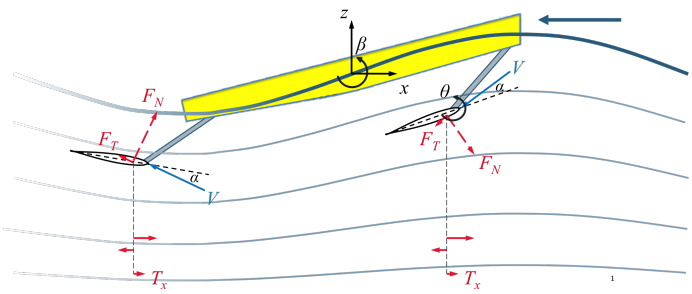

Figure 4: Schematic of the FLEUR system for ASV propulsion

The vessel heave (z_b), pitch (β) and pitch induced heave (z_β) contributes to the global position of a submerged foil and, hence, drives the motion of the foil through the water. A vessel with forward speed, U, in incoming head waves induces an incident flow stream with an equivalent velocity of U_∞ at the leading edge of the foil. Considering a quasi-steady approach, the flow over the foil is a combination of the incoming wave, the resulting vessel motions and the independent foil oscillations. Figure 4 illustrates the global frame of reference for the FLEUR system in the propulsion mode. The magnitude of the flow, V, and the angle of attack, α, are, therefore, evaluated as follows:

$$V = \sqrt{\left(U_\infty + u\right)^2 + \left(v - \dot{z}_b + \dot{z}_f + \dot{z}_\beta\right)^2}$$

$$\alpha = (\theta + \beta) - tan^{-1}\left(\frac{v - \dot{z}_b + \dot{z}_f + \dot{z}_\beta}{U_\infty + u}\right)$$

Through resolving the resultant hydrodynamic forces in the global frame of reference, it can be shown that the flapping foil system is capable of generating thrust. This phenomena has been investigated to improve the propulsive efficiency of ships in waves and applied to passively propel ASVs. In the same way, the FLEUR system takes advantage of wave induced vessel motions to generate propulsion utilizing submerged spring-loaded flapping foils. However, the design also incorporates the capability to recover wave energy for on-board power generation.

The submerged flapping foils are fixed to the hull abaft and beneath the bow via a rigid pivot arm of length, a, shown in Figure 4. In the propulsion mode, the foils are not free to heave independently of the vessel and zero power is recovered. By allowing the pivot arm to rotate about a point located near the keel line, the torque from the foils can apply mechanical work about the pivot point and recover power from the wave energy. In the power recovery mode, the foils are free to heave and pitch; restrained by a rotational viscous damper and rotational spring respectively. Assuming the rotational inertia and mass of the foil is negligible the equations of motion of a flapping foil pivoting about the leading edge and restrained by a rotational spring is simplified as follows:

$$\Sigma M_\theta = M_{c/4} - k_\theta\theta - \cancelto{0}{\xi_\theta\omega_\theta} \longrightarrow M_\theta = k_\theta\theta$$

where $M_{c/4}$ is the hydrodynamic moment about the hydrodynamic centre of the foil, assumed to be at one quarter of the chord from the leading edge. The rotational spring stiffness and damping constants for the leading edge and pivot arm are constant parameters; k and and ξ, respectively. Applying the same assumptions for the pivot arm but regarding it as a damped system the equation of motions can also be simplified as:

$$\Sigma M_\phi = F_\phi a - \cancelto{0}{k_\phi\phi} - \xi_\phi\omega_\phi \longrightarrow F_\phi a = \xi_\phi\omega_\phi$$

where F_ϕ is the resultant hydrodynamic force applied to the pivot arm by the flapping foils. Assuming, that the total loss of mechanical energy via the damper is converted into electrical energy, it is possible to regard the rotational damper as a generator. The power recovered by the system is the work done by the flapping foils over time:

$$P = \tau\omega = F_\phi a\omega_\phi = \xi_\phi{\omega_\phi}^2$$

III. Experimental Setup

An existing towing tank model has been modified for the purpose of the initial experiments. The model hull has been strengthened for testing in waves with the addition of a longitudinal stiffener, which also provides the housing for the flapping foil mounts. The general arrangement of the model is shown below in Figure 5 along with the corresponding model and foil particulars detailed in Table I.

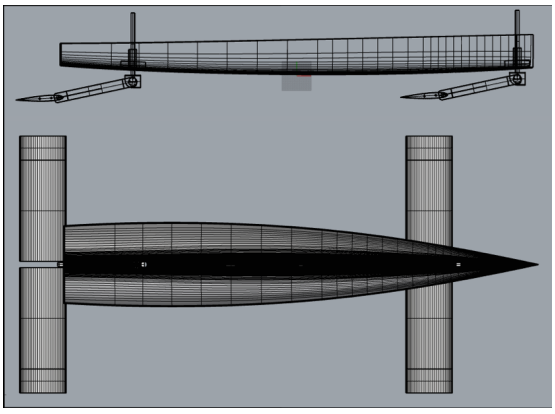

Figure 5: General arrangement of the experimental model

The model has been designed to accommodate the testing of various parameters and limit the added resistance incurred by the addition of appendages. The foils are fixed using vertical stainless steel tubes that protrude through the keel of the hull at the bow and abaft as shown in Figure 6. This setup provides

Table I: FLEUR ASV Particulars

Parameter	Value	Units
Length, L	2.27	m
Beam, B	0.3	m
Draft, T	0.1	m
Displacement, Δ	52	kg
Chord, c	0.23	m
Span, s	1	m
Foil type	NACA0012	-
Foil arm, a	0.4	m

the capability to alter the foil orientation and depth for further tests. The foils are mounted in two halves either side of the pivot arm and fixed via a shaft that rotates through three bearings that are pressed into the pivot arm, as can be seen in Figure 7.

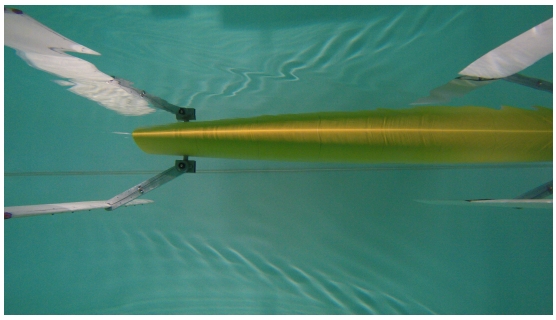

Figure 6: Underwater view of forward and aft foil setup

The spring constant can be altered using the same technique used by Bockmann et al. in their experiments to test the performance of a flapping foil under passive and active pitch conditions [19], illustrated in Figure 8. A length of spring steel is fixed to the foil rotational shaft either side of the bearing mounting, shown in Figure 7. The working length of the spring steel, d, can be adjusted by fixing the rod at different locations on the pivot arm, thus changing the spring constant. The centre of pitch can be set at the leading edge, one-quarter chord and half chord.

Figure 7: Pivot arm and rotational spring setup

For the purposes of the initial experiments the centre of pitch was located at the leading edge and the spring constant remained unaltered at a value of approximately 0.43 Nm/rad.

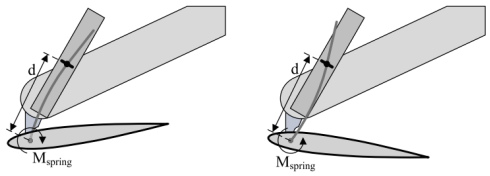

Figure 8: Pitch rotational spring setup used by Bockmann et al. [19]

By adjusting the height of the vertical mounting and setting the neutral pitch angle of the foil to 18^o relative to the pivot arm, shown in Figure 18 a) and Figure 19 a), the foil depth was set to 0.25m below the waterline. The foils are neutrally buoyant to prevent buoyancy forces or weight from applying a torque to the pivot arm. The depth of the foils was, therefore, maintained at 0.25m in the neutral condition.

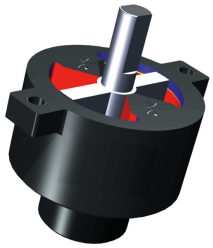

Figure 9: Cross section of the rotary damper

An adjustable rotational damper was used to constrain the rotary motion of the pivot arm. The damper is adjustable using a screw which alters the size of the orifice that the working fluid flows through to pass between the two reservoirs shown in Figure 9. Calibration experiments were conducted to calculate the damping constant values for the various screw settings. The number of turns from the highest damping setting (fully screwed) correlates to the damping constant as shown in Table II.

Table II: Damping constants calibration

No. of Turns	Damping constant, ζ / Nm/rads^{-1}
0	6.76
0.5	4.90
1	4.34
2	4.36

The angular position of the pivot arms were recorded using incremental magnetic rotary encoders rated to 1P68 protection. The signal outputs of the encoders were in the form of two quadrature sinusoidal analogue signals which can be interpolated to acquire the angular position and direction of rotation. The rotary damper and encoder are both mounted to a box section that form the pivot point and shaft connection for the pivot arm. The stainless steel box sections are welded to vertical stainless steel tubes through which the cables for the rotary encoders pass through to connect to the data

acquisition setup.

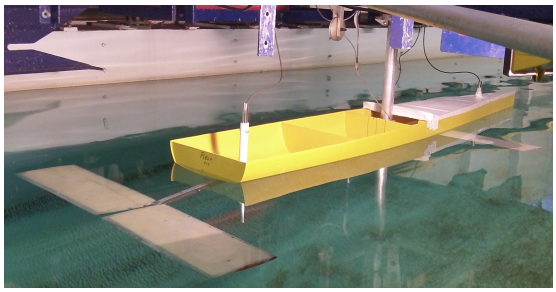

Figure 10: Carriage setup

The experiments were conducted at the Solent University towing tank. The tank is 60 m long, 3.7 m wide, 1.8m deep and has a wave generator capable of generating waves of upto 0.1 m in height at a frequency of upto 1 Hz. The model was fixed to the carriage via a tow post that is free to heave and allows the model to pitch, shown in Figure 10. Data was acquired for the wave height, vessel heave and pitch, drag and the angular position of the pivot arm. The experiments were carried out under three different conditions; bollard pull (zero carriage forward speed), towed condition and free running. For each condition the mode of the foils was altered at the pivot point through either fixing the pivot arm or applying a variable damping force by adjusting the rotary damper. In order to investigate the response of the foils and the vessel motions about the natural wave period in head waves, the system was tested over a series of increasing wave frequencies, from 0.4 to 1 Hz. No scaling laws were applied as the model is considered representative of a full scale ASV. Therefore, the frequency of waves generated in the tank are more representative of wind waves rather than ocean swell. For the majority of tests the wave height was kept constant at 0.08 m to maximise the hull motions whilst minimizing the amount of water ingress over the freeboard of the model.

IV. Results

A. Vessel motions

The pitch and heave motion of the model were interpreted by calculating the root square mean (RMS) of the time history for a range of wave frequencies, the results of which are found in Figures 11 and 12 respectively. The results reflect the expected response of a vessel that is exposed to head on regular waves of varying frequency [20]. The frequency is representative of wavelengths that exceed the length of the vessel (0.4 Hz - 9.8 m) to wavelengths less than that of the vessel length (1 Hz - 1.6 m).

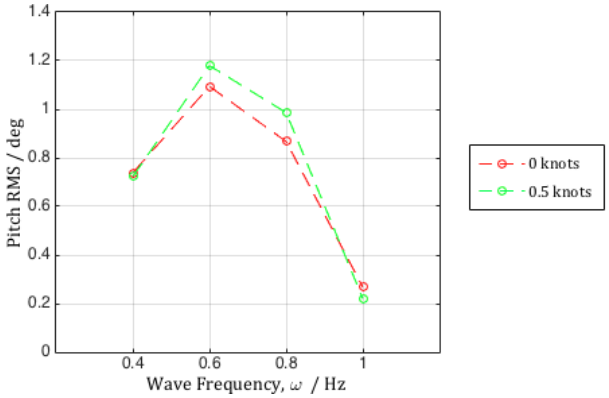

Figure 11: Pitch motion in waves of height, 0.08m.

It can be seen in Figure 11, that the resonant pitch response, in terms of pitch amplitude, is approximately equal to 0.6 Hz and the heave response of the model decreases with increasing wave frequency. With the increase of vessel speed from zero to 0.5 knots, we see that the model pitch motion increases but the heave does not change significantly.

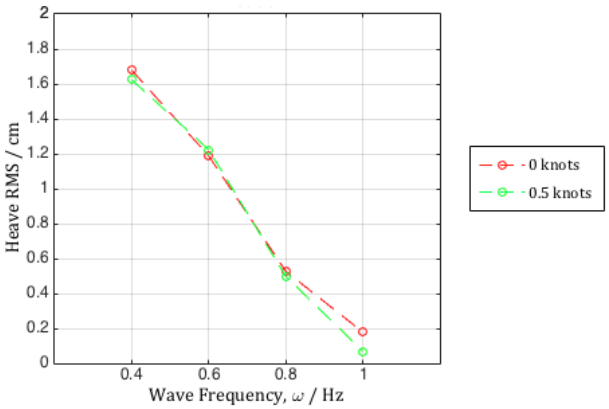

Figure 12: Heave motion in waves of height, 0.08m.

Figure 13 shows the RMS pitch response of the model whilst fixed to the carriage at zero speed under different conditions. Fixed foils mounted at the bow and stern of the vessel significantly reduces the pitch motions when compared to the pitch motion of the model with a bare hull. In the condition where the foils are free to heave the vessel pitch motion decreases with the increase of pivot arm damping.

B. Propulsion

Figure 14 shows the bollard pull of the foils when the carriage was stationary and the reduction of drag when the carriage had a forward speed of 0.5 knots. Both sets of results identify that there is an optimum frequency of approximately 0.8 Hz; at which the foils generate thrust due to the combined vessel motions at this frequency. The flapping mechanism of the foils that leads to the generation of thrust is captured in the underwater snapshots shown in Figures 18 and 19 for the aft and forward foils respectively. In experiments where the foils were free to heave but restrained by a rotary damper, the

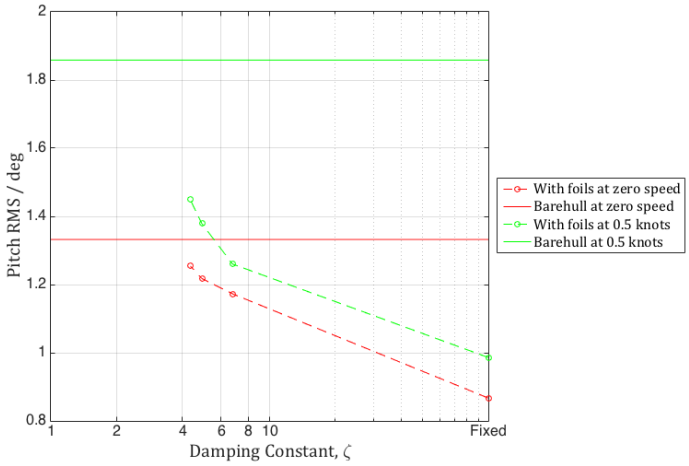

Figure 13: Influence of relative foil motions on the pitch of the model in waves of height, 0.08m, and frequency, 0.8 Hz

flapping foils generated zero thrust. This was also confirmed in the free running tests and is most likely due to the relatively low damping applied to the pivot arm.

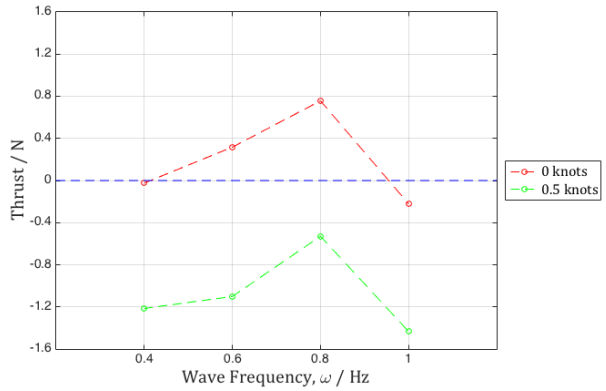

Figure 14: Thrust generation in waves of height 0.08m

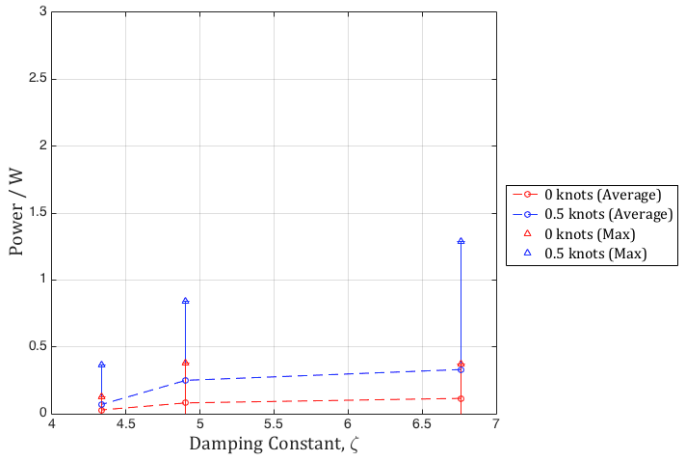

Figure 15: Forward foil maximum and average power with varying damping constant in waves of frequency, 0.8 Hz and height, 0.08m.

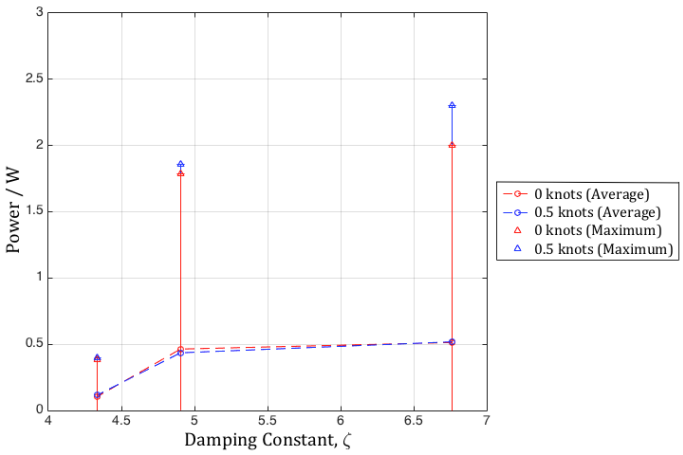

Figure 16: Aft foil maximum and average power with varying damping constant in waves of frequency, 0.8 Hz and height, 0.08m.

C. *Power Generation*

By adjusting the damping settings, detailed in Table II, it was possible to assess the effect of foil heave on the power generated. Figures 15 and 16 show the maximum and average power generated by the forward and aft foil respectively. Both figures present a trend showing the increase of power generation with the increase in damping.

Drawing comparisons between Figures 15 and 16 it is apparent that the forward foil generates less power than the aft foil. The foils are not located equidistant from the longitudinal centre of rotation (the tow post fitting in this case). Consequently, the pitch induced heave is significantly less for the forward foil and, therefore, the rate at which the forward foil heaves relative to the vessel is less than that of the aft foil.

Figure 17 shows the time history of foil heave, pivot arm angular velocity and the equivalent power generated by the aft foil at zero speed in an incoming wave of height, 0.08 m, and frequency, 0.8 Hz with the damping setting at 0. The foil heave was evaluated from the rotational data acquired by the rotary encoder using basic trigonometry. The results show an increase in foil response as the wave height progresses from zero to 0.08 m. The foil is seen to start at an initial depth slightly shallower than its neutral position before settling into a steady oscillation about the neutral position. The cyclic response of the foil is reflected in the power generated at the rotary damper.

The power generated by the aft foil is seen to peak within each cycle at the point where the foil is plunging/heaving at its maximum velocity through the neutral heave position. The peak power is not sustained as the foil is encouraged to oscillate within the same period as the wave induced motions of the model. The results present a promising generation of power, upto a maximum of 2 watts per foil, and proves that it is possible to recover wave energy using flapping foils onboard

ASVs.

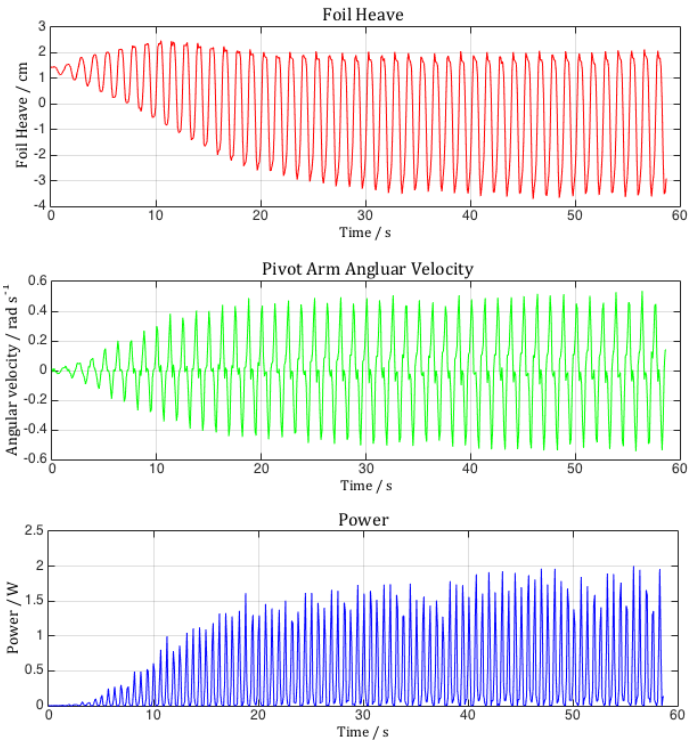

Figure 17: Foil motions and power generation time history at zero speed on damping setting 0 in an incoming waves of height,0.08 m, and frequency, 0.8 Hz.

D. Free running

Free running tests were carried out in the towing tank to assess the performance of the FLEUR system without the constraining effects of fixing the model to the carriage. The model was located in the centre of the tank and exposed to head on regular waves with a frequency of 0.8 Hz and two different heights; 0.1 m and 0.08 m. Posts, which were situated every 3 m along the tank, were used to clock the average speed of the model in 3 m intervals. With the foils fixed, the model achieved a maximum forward speed of approximately 0.43 knots and 0.27 knots for wave heights of 0.1 m and 0.08 m, respectively. The model was also tested with the foils free to heave on the damping setting of 1 turn. In this scenario, the vessel held station in both sets of wave heights and was assumed to be generating power. However, no data was acquired as running cables back to the data acquisition hardware on the carriage was not feasible. Using results acquired on the carriage from previous tests it maybe assumed that the aft foil was generating a maximum of approximately 1.7 W and 0.4 W in waves of 0.1 m and 0.08 m respectively. The damping setting used in this instance was much less than optimal and further experiments are required to optimize this aspect of the FLEUR system.

V. Discussion

In comparison to most seakeeping analysis, large wave induced vessel motions are a desired characteristic for the FLEUR system. Maximising the combined pitch and heave motions drives the foils through the water to generate thrust from the flapping foils. The model was initially tested in wave heights of 0.1 m to maximise the vessel motions. However, there was a risk of water ingress and it was identified that the wave height significantly contributed to the added wave resistance. It was, therefore, concluded that solely maximising the vessel motions will not produce the optimum propulsive performance as the added wave resistance needs to be considered. The coupled foil and vessel added wave resistance was not evaluated in this set of experiments but will be a critical area for future research.

The motions of the entire system are coupled so that the foils absorb energy from the incoming waves and, hence, result in a reduction in the vessel motion. This feedback in the coupled system reduces the propulsive gain made by the flapping foils. It is, therefore, possible to design an optimal foil chord length for a particular vessel where there is a peak in propulsive performance. Evaluating the foil chord length is particularly important for optimizing the performance of the FLEUR system in irregular waves as well as waves in various headings. The initial experiments have been conducted in waves that are assumed to provoke the optimal response from the system and further experiments are required to assess its performance in a variety of different sea states and headings. The effect of fixing the model to the carriage impedes the natural behaviour of coupled system and consequently the results may have underestimated the thrust generated by the foils.

Allowing the foils to independently heave relative to the model significantly reduced their propulsive performance. This may have been due to a slight backlash in the rotary damper that permitted a few degrees of free motion irrespective of the applied damping setting. This slight backlash made it difficult to investigate the possibility of simultaneous thrust and power generation. Further enhancements in propulsive performance may also be made by changing the pitch spring constant as highlighted by Bockmann et al.[19].

The range of damping applied in these experiments did not encompass the optimum damping constant for power generation which indicates that the value of applied damping from the rotary damper was too low. However, the uncertainty associated with backlash is difficult to quantify and improvements to the method for simulating power take-off is necessary.

In the free running tests, the damping setting was set to 1 turn which applies a damping constant that is too low for the system to effectively recover power from the incoming waves. The power generated in this study was not harvested or stored and the development of a power take-off device is required. However, the results indicate that it is possible to gain net power and thrust from the same system. Improving the model to allow for more advanced testing under free running

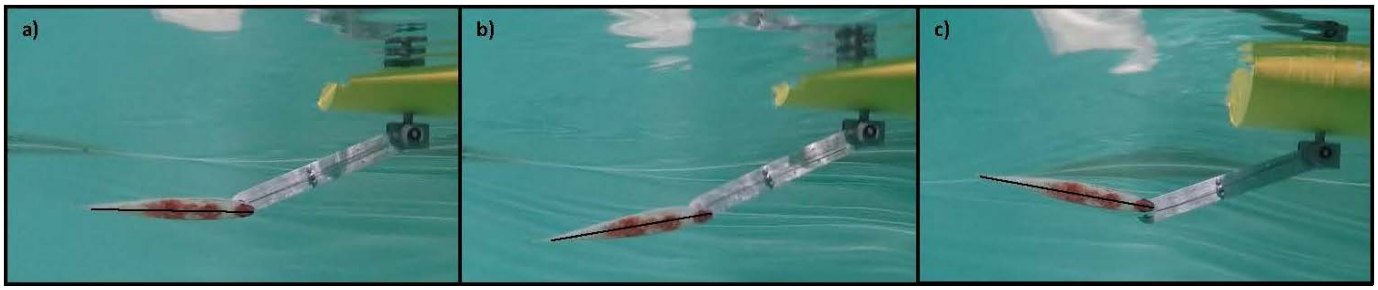

Figure 18: Aft foil spring loaded motion: a) Neutral Angle b) Positive Pitch c) Negative Pitch

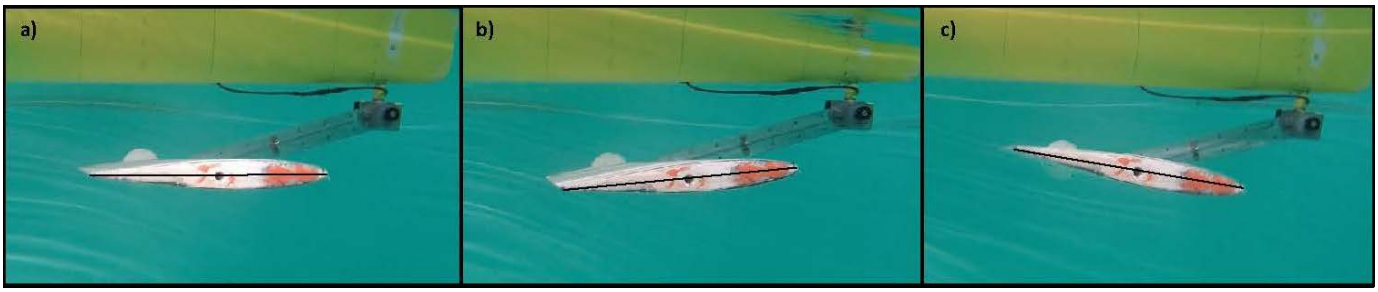

Figure 19: Forward foil spring loaded motion: a) Neutral Angle b) Positive Pitch c) Negative Pitch

conditions is seen as a key objective for future research.

VI. Conclusions

The ability to alter the mode of flapping foils from ASV propulsion to onboard power generation has been outlined and proven from these initial experiments. The mode of the flapping foils was changed from propulsion to power generation by allowing the foils to heave independently from the vessel and, therefore, recover wave energy in the form of work done about the rotary damper. Thrust was generated in the form of bollard pull, forward speed and drag reduction. In the power generation mode, the results showed that a maximum of approximately 4 watts and an average of 1 watt is attainable from two sets of foils. Upon optimization, the FLEUR system could recover a useful amount of power for ASV onboard systems and introduce the flexibility required to remotely control and alter the ASV mission directive such as station holding, charging, transiting and evading.

VII. Further work

Further experiments are required to improve the range of damping required to analyze the simultaneous generation of power and thrust from the system. Linear dampers have been proposed as a more effective means of adjusting and applying damping to the pivot arms. It was also identified that fixing the system to the towing tank carriage may have limited the response and overall performance of the system. Hence, future experiments should be carried out in a free running condition where the model is remotely operated in the towing tank and data is acquired onboard. Ideally, this would also incorporate the ability to remotely change the mode of the flapping foils. Furthermore, the FLEUR system could incorporate the ability to use stored energy to actively drive the flapping foil system and consequently propel itself in circumstances where no wave energy is available or an increase in vessel speed is required.

Acknowledgements

This research was supported by the Lloyd's Register Foundation.

References

[1] Manley, Justin E. "Unmanned surface vehicles, 15 years of development." OCEANS 2008. IEEE, 2008.

[2] Zheng, C., Shao, L., Shi, W., Su, Q., Lin, G., Li, X. and Chen, X.,"An assessment of global ocean wave energy resources over the last 45 a", Acta Oceanologica Sinica, vol. 33(1), pp 92-101, 2014.

[3] Manley, Justin, and Scott Willcox. "The wave glider: A persistent platform for ocean science." OCEANS '10 IEEE-Sydney. IEEE, 2010.

[4] D. Crimmins, C. Patty, M. Beliard, J. Baker, J. Jalbert, R. Komerska, S. Chappell, and D. Blidberg, Long-endurance test results of the solar powered AUV system, OCEANS 06, pp. 15, 2006.

[5] Saildrone Inc, March 2015, accessed March 2015, http://www.saildrone.com/

[6] Martins, Alfredo, et al. "ROAZ and ROAZ II autonomous surface vehicle design and implementation." International Lifesaving Congress. 2007.

[7] MOST (AV) Ltd, accessed March 2015, ¡http://www.autonautusv.com/specifications

[8] ASV Global, accessed March 2015, http://www.asvglobal.com/science-survey

[9] Linden, H. ”Improved combination with floating bodies, of fins adapted to effect their propulsion”. GB Patent 14,630. Filed Aug. 1, 1895. Patented Jul. 18, 1896.

[10] Jakobsen, E., ”The foil propeller, wave power for propulsion”. In Second International Symposium on Wave and Tidal Energy, BHRA Fluid Engineering, pp 363369, 1981.

[11] Terao, Y., and N. Sakagami. ”Design and development of an autonomous wave-powered boat with a wave devouring propulsion system.” Advanced Robotics, vol. 29(1), pp 89-102, 2015.

[12] Townsend, N.C. and Shenoi, R.A., ’Recharging autonomous underwater vehicles from ambient wave induced motions’, OCEANS13, MTS/IEEE, San Diego September 23rd - 26th, 2013.

[13] Isshiki, H. and Murakami, M., ”A Theory of Wave Devouring Propulsion(4th Report) : A Comparison Between Theory and Experiment in Case of a Passive-Type Hydrofoil Propulsor”, Journal of the Society of Naval Architects of Japan, vol. 156, pp. 102-114, 1984.

[14] Wu, T. Y., ’Extraction of flow energy by a wing oscillating in waves’, Journal of Ship Research, vol. 14(1), pp 66-78, 1972

[15] Grue, J., Mo, A. and Palm, E., ”Propulsion of a foil moving in water waves”, Journal of Fluid Mechanics, vol. 186, pp 393-417, 1988

[16] Filippas, E. S. and Belibassakis, K. A., ”Hydrodynamic analysis of flapping-foil thrusters operating beneath the free surface and in waves”, Engineering Analysis with Boundary Elements, vol. 41(0), pp 47-59, 2014.

[17] Young, J., Lai, J. C. S. and Platzer, M. F., ”A review of progress and challenges in flapping foil power generation”, Progress in Aerospace Sciences, vol. 67(0), pp 2-28, 2014.

[18] Jones, K. and Platzer, M., ”Numerical computation of flapping-wing propulsion and power extraction”, In 35th Aerospace Sciences Meeting and Exhibit, American Institute of Aeronautics and Astronautics, 1997.

[19] Bockmann, E and Steen, S, ”Experiments with actively pitch-controlled and spring-loaded oscillating foils”, Applied Ocean Research, vol. 48, pp 227-335, 2014.

[20] A. R. J. M. Lloyd, ”Seakeeping: ship behaviour in rough weather”, Ellis Horwood Series in Marine Technology, Ellis Horwood Limited, Chapter 13, 1989.